

Vanadocene as a Temperature Standard for ^{13}C and ^1H MAS NMR and for Solution-State NMR Spectroscopy

Frank H. Köhler* and Xiulan Xie†

Anorganisch-chemisches Institut, Technische Universität München, D-85747 Garching, Germany

Paramagnetic vanadocene gives easily recordable ^1H and ^{13}C solid-state NMR signals which are shifted by more than 300 and 500 ppm (to high and low frequency, at room temperature), respectively. The strong temperature dependence of these shifts is the basis of new NMR signal shift thermometers for solutions and for the solid state. Since different signal shifts are found for the two states, primary referencing is established by using a resistance thermometer for solutions and absorbed glycol for the solid state. In the MAS experiment the sample temperature, T_s , depends linearly on the temperature set on the controller, as verified for five rotor spinning rates, ν_r , between 6 and 12 kHz. The slope and the intercept of the calibration curves depend on ν_r . In a T_s vs. ν_r^2 plot, a non-linear correlation is found. In addition to ^1H , ^{13}C is a useful nucleus for measuring T_s . With simple spectrometer handling and favourable signal shift data, vanadocene meets the requirements of an internal temperature standard for MAS NMR studies.

Magn. Reson. Chem. 35, 487–492 (1997) No. of Figures: 5 No. of Tables: 2 No. of References: 13

Keywords: ^1H MAS NMR; ^{13}C MAS NMR; shift thermometer; vanadocene

Received 16 December 1996; revised 18 February 1997; accepted 25 February 1997

INTRODUCTION

The measurement of the sample temperature in solid-state NMR spectroscopy has been addressed more than 10 years ago,¹ and yet it is still being studied intensively in many laboratories.² The reason is that, as solid-state NMR becomes widely applied, an increasing number of temperature-dependent phenomena^{2h,k} are being investigated. The precise temperature and the reproducibility of the NMR experiment depend on a number of factors such as the design of the probe head, the material and the size of the rotor, the weight of the sample, the pressure and the nature of the bearing and drive gas, the Joule–Thompson effect and the spinning speed of the rotor. Some of these factors are correlated, and a temperature gradient in the sample must also be considered.

Given these influences and the fact that different nuclei are to be studied, the all-purpose temperature standard will be difficult to realize. Rather, various user-adapted versions are envisaged. There are several illuminating studies on chemical-shift thermometers that use the nuclei ^1H ,^{2a,e,f} ^{13}C ,¹ ^{15}N ,^{2b} ^{31}P ,^{2c} ^{119}Sn ,^{2d,g,l} and ^{207}Pb ,^{2h–j} well defined solid–solid^{1,2d,g,k} and solid–liquid^{2m} phase transitions that are detectable by NMR

spectroscopy were also employed. In any case, the basic question is how reliable the primary calibration is. As emphasized by Riddell *et al.*^{2k} recently, a major advantage of the phase transition method is that the absolute reference temperatures are precisely known. The method would further benefit from clarifying the effect of spinning-induced pressure changes and gradients on the phase transition and also from reducing the apparent temperature range in which two phases are seen in the spectrum. As for the latter problem, promising examples were reported by van Moorsel *et al.*^{2g}

We became aware of the temperature variation when we recorded the ^1H and ^{13}C NMR spectra of solid chromocenes,³ which have two unpaired electrons. Clearly, their signal shifts and related information such as spin densities and deviations from the Curie law are only meaningful when the temperature is known. Desirable requirements for temperature measurements of our samples, similar to a plethora of organic and organometallic samples, were the following. (i) The sensor should be utilizable as external and internal (i.e. admixed with the sample) standard. The latter purpose would be difficult to achieve with the phase-transition method. (ii) When using a chemical-shift thermometer, the temperature should be related to a shift difference rather than to an absolute shift that would be more difficult to reproduce. This would set aside the above-mentioned thermometers described for ^{13}C , ^{15}N , ^{31}P and ^{207}Pb . (iii) Circuit retuning due to frequency changes for reading an internal shift thermometer should be avoided for convenience. When studying the

† On leave from the Fujian Institute of Research on the Structure of Matter, Chinese Academy of Science, Fuzhou Fujian, China.

* Correspondence to: F. H. Köhler.

Contract grant sponsor: Fonds der Chemischen Industrie.

most popular nucleus, ^{13}C , this would render thermometers based on nuclei other than ^{13}C (and ^1H ; see below) less suitable. (iv) The mechanical risk while working routinely with rotor spinning rates far above 10 kHz should be low. Therefore, we did not want to apply thermometers that use alcohols in a capillary or mixed with solids^{2a,f,h} at high spinning rates.

Here we suggest vanadocene (Cp_2V ; Cp = cyclopentadienyl) as a ^1H and ^{13}C MAS NMR temperature standard that may be applied both externally and internally.

RESULTS AND DISCUSSION

Solid-state NMR spectra of vanadocene

The sandwich compound Cp_2V can be purchased or synthesized in high yield and large quantities.⁴ Because of the presence of three unpaired electrons, the molecule has large ^1H and ^{13}C NMR shifts in solution that depend strongly on the temperature.⁵ Thus, at room temperature the ^1H and ^{13}C NMR signals appear near

320 and -510 ppm, respectively. The temperature is related to a shift difference when Cp_2V is combined with the isostructural ferrocene (Cp_2Fe). Choosing Cp_2Fe as a reference is particularly useful, because it eliminates the signal shift that Cp_2V would have if it were diamagnetic. We are thus left with the paramagnetic shift (δ^{para}) that exclusively reflects the effect of the unpaired electrons. In solution $1/\delta^{\text{para}}(^1\text{H})$ behaves as T whereas $1/\delta^{\text{para}}(^{13}\text{C})$ deviates somewhat.⁵ The inverse magnetic susceptibility of solid Cp_2V is also proportional to T .⁶ This would allow the cross-checking of the temperature calibration of the solid-state ^1H NMR data for Cp_2V .

Typical spectra of the couple $\text{Cp}_2\text{V}/\text{Cp}_2\text{Fe}$ are reproduced in Fig. 1. The comparison of traces A and B demonstrates that a mechanically mixed sample (B), which is more easily obtained than a co-sublimed sample (A), is sufficient to obtain a good signal-to-noise (S/N) ratio within about 3 min. The ^{13}C NMR spectrum (C), which might also be used as a thermometer, was obtained after 1.5 h. Accidentally, at a spinning rate of 12 kHz the sideband manifolds of Cp_2V and Cp_2Fe almost coincide. It is also evident that a high spinning rate is advantageous for reducing the number of sidebands, thus increasing the S/N ratio and facilitating spectral analysis. Actually, unpaired electrons not only

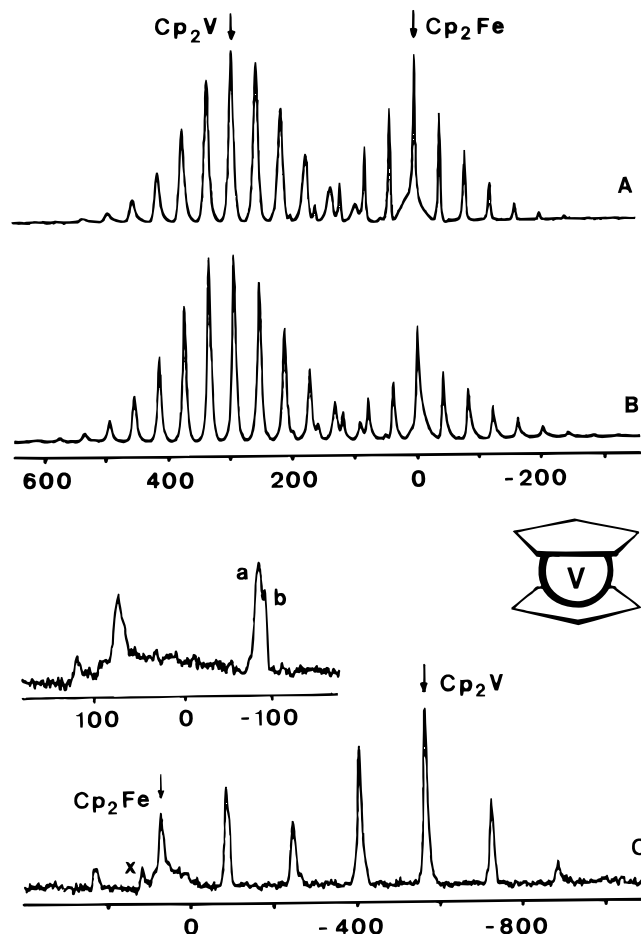


Figure 1. MAS NMR spectra of mixtures of Cp_2V and Cp_2Fe . Rotor spinning rate 12.0 kHz; scales in ppm relative to TMS. (A) ^1H NMR, co-sublimed sample with ca. 40% of Cp_2Fe , 298.0 K. (B) ^1H NMR, mechanically mixed sample with 15% of Cp_2Fe , 297.5 K. (C) ^{13}C NMR after subtraction of background signal, conditions as in B, X = impurity; inset, range $-180 < \delta < 180$ expanded; a = third sideband of Cp_2V and b = first sideband of Cp_2Fe .

contribute to the total width of the signal pattern of the paramagnetic species itself,⁷ but also to that of admixed diamagnetic species,⁸ in this particular case Cp_2Fe .

^1H NMR spectra like those shown in Fig. 1 can be recorded by using the decoupling channel of most MAS probe heads. Obviously then, a small amount of $\text{Cp}_2\text{V}/\text{Cp}_2\text{Fe}$ mixed with the sample of interest (or separated from it by a thin spacer that would prevent conceivable reactions) can serve as an internal temperature standard in variable-temperature studies of other nuclei. The principle is demonstrated in Fig. 2, where the spectrum of cobaltocene (spin 1/2) was recorded at the temperature indicated by the signals of $\text{Cp}_2\text{V}/\text{Cp}_2\text{Fe}$. Note that the ^{13}C MAS NMR spectra of diamagnetic compounds, the most frequent case, are not complicated by the internal thermometer because of the large ^{13}C NMR signal shift of Cp_2V .

^1H NMR of $\text{Cp}_2\text{V}/\text{Cp}_2\text{Fe}$ at variable temperature

As already stated, it is not trivial to determine the intercept in a chemical shift *vs.* temperature diagram, i.e. to link the correlation to the absolute temperature. The $\text{Cp}_2\text{V}/\text{Cp}_2\text{Fe}$ couple was chosen because a very precise measurement (sophisticated laboratory-made insert with liquid heating medium,^{9a} calibrated precision thermometer) was carried out by Dietrich and Ulbrich.^{9b} To our surprise, we found no significant deviation from that calibration curve when calibrating our spectrometer equipped with a commercial probe head (Experimental). It is also gratifying that our previous data, obtained with yet another spectrometer,⁵ fit well with the curve given in Fig. 3. However, when solid $\text{Cp}_2\text{V}/\text{Cp}_2\text{Fe}$ was investigated at low spinning rates and 298 K, a significant difference of the ^1H NMR signal shift in solution and in the solid state was observed. This was quantified by using the glycol/tetrakis(trimethylsilyl)silane (TTMSS) thermometer^{2f} (cf. Experimental), because external thermometers are not reliable in solid-state NMR spectroscopy. A temperature series of the glycol/TTMSS and the $\text{Cp}_2\text{V}/\text{Cp}_2\text{Fe}$ samples under identical conditions (same rotor, same bearing and drive gas pressures) at a rotor spinning rate of $\nu_r = 6.0$ kHz gave the following correlations for $\text{Cp}_2\text{V}/\text{Cp}_2\text{Fe}$ (T_s = sample temperature in

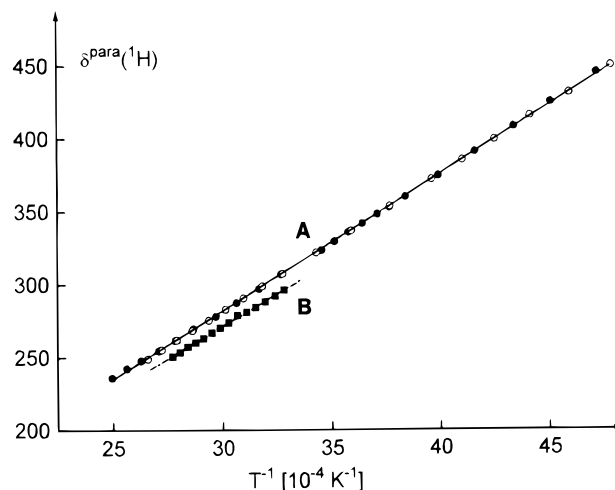


Figure 3. Temperature dependence of the paramagnetic ^1H NMR signal shift of Cp_2V (A) in toluene and (B) in the solid state. Rotor spinning rate, 6.0 kHz. ●, ■, This work; ○, Ref. 5.

K):

$$\text{solution: } T_s = 9.423 \times 10^4 / \delta^{\text{para}}(^1\text{H}) - 0.97 \quad (1)$$

$$\text{solid: } T_s = 9.228 \times 10^4 / \delta^{\text{para}}(^1\text{H}) - 7.06 \quad (2)$$

The signal shifts at 298 K were $\delta^{\text{para}}(^1\text{H}, \text{solution}) = 315.2$, $\delta^{\text{para}}(^1\text{H}, \text{solid}) = 302.5$ and $\Delta\delta^{\text{para}}(^1\text{H}) = 12.7$. This difference points to intermolecular interactions. Indeed, we have observed previously that paramagnetic ^1H and ^{13}C NMR shifts depend on the concentration of the sample and, to explain this, we have considered intermolecular dipolar and susceptibility shifts of the signals.¹⁰ It can be seen in Fig. 3 that the Curie behavior is not affected when passing from solution to the solid state as would be expected from the susceptibility data⁶ in the corresponding temperature range.

The solid-state NMR shift-temperature correlation [Eqn (2)] was used to extend the temperature calibration to higher spinning rates. The data for five variable-temperature series were fitted to the equation

$$T_s = AT_c + B \quad (3)$$

where T_c is the temperature set at the controller (i.e. of the bearing gas). The results are collected in Table 1.

Inspection of Table 1 reveals that there is a perfect linear relationship between T_s and T_c . However, additional trends emerge that must be considered when changing the experimental set-up, as follows.

(i) The slope A of the calibration curves [cf. Eqn (3)] decreases when ν_r increases. This is ascribed to the fact that the drive gas is at room temperature, whereas the temperature of the bearing gas is controlled. Their pressures, P_d and P_b , respectively, are also given in Table 1. It is evident that, generally, T_s will be influenced increasingly by P_b as ν_r increases and as we depart from room temperature. In the present study, the P_d/P_b ratio increases (almost linearly) with ν_r ³ near 300 K, while for a given ν_r it drops by roughly 10% on heating to 370 K. As a net result, T_s is lowered, and this effect is biggest at $\nu_r = 12$ kHz and at high T_c .

(ii) The intercept B of the calibration curves also varies with ν_r . Actually, this variation must be corrected

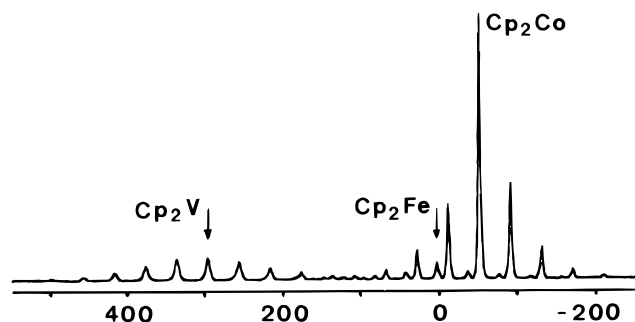


Figure 2. ^1H MAS NMR spectrum of $\text{Cp}_2\text{Co}/\text{Cp}_2\text{V}/\text{Cp}_2\text{Fe}$ (70:25.5:4.5) at 341.2 K. Rotor spinning rate 12.0 kHz; scale in ppm relative to TMS.

Table 1. Temperature calibration of the MAS probe-head^a: parameters of the fit to Eqn (3) and auxiliary gas data

| Parameter | Spinning rate, ν_r (kHz) | | | | | |
|---------------------|------------------------------|-------|-------|-------|-------|-------------------|
| | 6.0 | 7.5 | 9.0 | 10.5 | 12.0 | 12.0 ^b |
| A | 0.876 | 0.876 | 0.877 | 0.867 | 0.845 | 0.855 |
| B | 36.7 | 37.9 | 38.7 | 43.7 | 53.6 | 52.6 |
| T_d | 298.0 | 295.5 | 296.0 | 295.5 | 297.0 | 296.5 |
| B_{corr}^c | 0.123 | 0.128 | 0.131 | 0.148 | 0.181 | 0.177 |
| P_d (mbar) | 390 | 600 | 850 | 1160 | 1520 | 1540 |
| P_b (mbar) | 2440 | 2880 | 2980 | 2940 | 2960 | 2940 |
| P_d/P_b | 0.160 | 0.208 | 0.285 | 0.395 | 0.514 | 0.524 |

^a Temperature range 305–370 K, 14 data points per ν_r , correlation coefficient $r = 0.9999$; Si_3N_4 rotor, sample weight 546.5 mg except where indicated.

^b ZrO_2 rotor, sample weight 818.2 mg.

^c $B_{\text{corr}} = B/T_d$.

for the temperature of the drive gas, T_d (cf. Table 1), yielding B_{corr} . As expected from frictional heating of the rotor (see below), B_{corr} depends on the rotor spinning rate. It is worth mentioning that B_{corr} does not increase linearly with ν_r^2 .

(iii) The 12 kHz entry in Table 1 shows that the slope A of the calibration curve increases on passing from an Si_3N_4 to a ZrO_2 rotor of the same size, similarly to the ν_r -dependent study below. By contrast, B decreases slightly. Finally, thermal equilibrium is reached more quickly in the Si_3N_4 rotor (see Experimental) owing to the thermal conductivity, which is roughly 20 times better than that of ZrO_2 .¹¹ High-power proton decoupling does not change the sample temperature. This is consistent with Ferguson and Haw's recent report^{2m} which shows that efficient rotor heating is only achieved after coating with platinum, and that the heat is dissipated rapidly.

¹H NMR of $\text{Cp}_2\text{V}/\text{Cp}_2\text{Fe}$ at variable rotor spinning rate

From previous studies,^{2a,d,e,j,l,3,12} it is known that at a given temperature setting of the controller the sample temperature increases when the rotor spins faster. This was also observed in the last section. Since the temperature calibration was limited to five spinning rates, we checked the ν_r dependence of our set-up separately. The result is shown in Fig. 4, which shows that the heating is more pronounced for the ZrO_2 than the Si_3N_4 rotor. Differences were also observed for Al_2O_3 , Si_3N_4 and ZrO_2 rotors during ^{15}N and ^{207}Pb NMR studies by Aguilar-Parrilla *et al.*¹² and van Gorkom *et al.*,^{2h} respectively.

As for a data fit, it was reasonable to suggest first Eqn (4), because the heating was traced to rotor friction.¹² Later it turned out that T_s vs. ν_r^2 plots did not give straight lines, and equations of type (5) and (6) were put forward by Anderson-Altmann and Grant^{2e} and Grimmer *et al.*,²¹ respectively:

$$T_s = a\nu_r^2 + d \quad (4)$$

$$T_s = a\nu_r^2 + b\nu_r^4 + d \quad (5)$$

$$T_s = a\nu_r^2 + c\nu_r + d \quad (6)$$

Fitting of the experimental data to these equations gave the results in Fig. 4 and Table 2. The curves obtained for Eqns (5) and (6) were very similar; therefore, only one is given in Figure 4. Obviously, Eqn (4) is

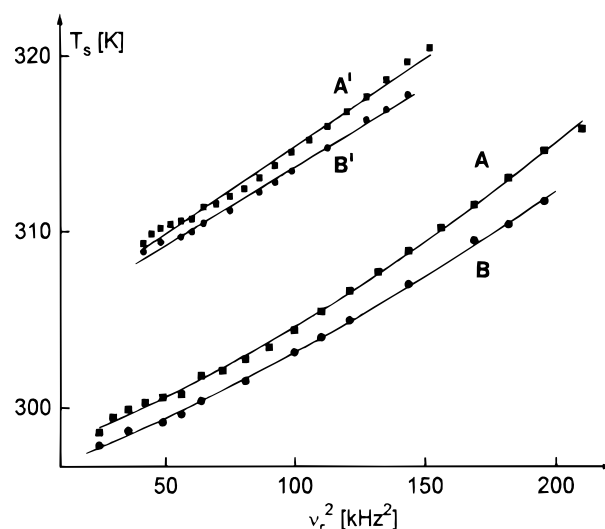


Figure 4. Dependence of the sample temperature on the rotor spinning rate. Rotor material (A, A') ZrO_2 and (B, B') Si_3N_4 . The data were fitted to Eqn (5), yielding curves A and B, and to Eqn (4), yielding curves A' and B' (inset, scales do not apply).

Table 2. Dependence of sample temperature on rotor spinning rate: comparison of the fit of the experimental data to Eqns (4), (5) and (6)^a

| Eqn | Rotor | Fit parameters | | | | |
|-----|-------------------------|----------------------|----------------------|-------|-------|--------|
| | | a | b | c | d | r^b |
| (4) | ZrO_2 | 9.2×10^{-3} | | | 295.9 | 0.9955 |
| | Si_3N_4 | 8.3×10^{-3} | | | 295.2 | 0.9975 |
| (5) | ZrO_2 | 5.1×10^{-3} | 1.9×10^{-4} | | 297.6 | 0.9993 |
| | Si_3N_4 | 5.8×10^{-3} | 1.1×10^{-4} | | 296.2 | 0.9994 |
| (6) | ZrO_2 | 0.156 | | -1.26 | 301.5 | 0.9991 |
| | Si_3N_4 | 0.125 | | -0.82 | 298.9 | 0.9997 |

^a For ν_r in kHz and T_s in K.

^b Regression coefficient.

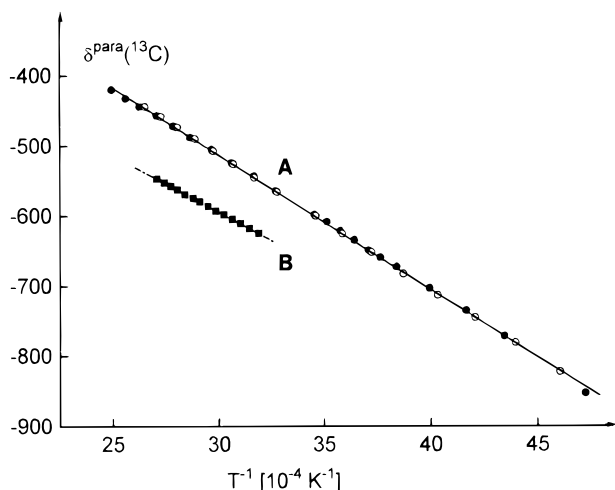


Figure 5. Temperature dependence of the paramagnetic ^{13}C NMR signal shifts of Cp_2V (A) in toluene and (B) in the solid state. Rotor spinning rate 12.0 kHz. ●, ■, This work; ○, Ref. 5.

less satisfactory than are Eqns (5) and (6), although the physics behind the latter remain to be clarified. As for the paramagnetic NMR signal shift, δ^{para} , of a shift thermometer, it should be a non-linear function of ν_r . This was confirmed by our data; in narrow ranges of ν_r the $\delta^{\text{para}}-\nu_r$ correlation might look linear.^{2d}

^{13}C NMR of $\text{Cp}_2\text{V}/\text{Cp}_2\text{Fe}$ at variable temperature

From Fig. 1(C), it follows that the ^{13}C NMR signals of $\text{Cp}_2\text{V}/\text{Cp}_2\text{Fe}$ could also serve as a MAS NMR thermometer. We checked this for $\nu_r = 12.0$ kHz and linked the ^{13}C to the ^1H NMR shift thermometer (Table 1) by switching the nuclei at a given T_c . The result is shown in Fig. 5, together with the calibration which was obtained for a solution of $\text{Cp}_2\text{V}/\text{Cp}_2\text{Fe}$ in toluene on 7.05 and 4.70 T⁵ spectrometers. The data fit yielded

$$\text{solution: } T_s = -15.521 \times 10^4 / \delta^{\text{para}}(^{13}\text{C}) + 29.68 \quad (7)$$

$$\text{solid: } T_s = -24.243 \times 10^4 / \delta^{\text{para}}(^{13}\text{C}) - 74.42 \quad (8)$$

and the signal shifts at 298 K were calculated to be $\delta^{\text{para}}(^{13}\text{C}, \text{solution}) = -578.5$, $\delta^{\text{para}}(^{13}\text{C}, \text{solid}) = -651.0$ and $\Delta\delta^{\text{para}}(^{13}\text{C}) = 72.5$. Although this shift difference is rather large, it is not unexpected, since the above-mentioned concentration dependence of the paramagnetic shifts in solution is more pronounced for ^{13}C than for ^1H .¹⁰

The comparison of the $\text{Cp}_2\text{V}/\text{Cp}_2\text{Fe}$ ^1H and ^{13}C NMR shift thermometers reveals that ^{13}C is more precise (1.8 ppm K^{-1} for ^{13}C and 1.0 ppm K^{-1} for ^1H at 298 K), while ^1H is more rapid.

CONCLUSION

The vanadocene/ferrocene couple proves to be a precise signal shift thermometer for NMR experiments in both the solution and the solid states. It is not only applic-

able for the most common nuclei ^1H and ^{13}C , but is anticipated to work also for all other nuclei when the probe-head has a proton decoupling channel.

The temperature *vs.* shift calibration in this work may be used in other laboratories for solution-state studies without change. By contrast, a recalibration may be necessary for solid-state NMR work when different probe-heads, rotor materials, sample weights, heating devices and the like are used. The vanadocene/ferrocene couple may be also applied as an internal temperature standard. Then the correlations given in Eqns (2) and (8) replace all recalibrations.

EXPERIMENTAL

Solid-state ^1H and ^{13}C MAS NMR spectra were recorded on a Bruker MSL 300 spectrometer (operating at 300.13 and 75.47 MHz, respectively) by using a 4 mm standard Bruker double air-bearing probe-head. Dry nitrogen was used as drive and bearing gas; the temperature of the latter was controlled by a BVT 1000 (Eurotherm) unit. Its thermocouple was placed at the bearing gas outlet of the probe-head, and hence the temperature set and measured at the controller (T_c) was the bearing gas temperature. Since the same source supplied the drive and the bearing gas, their temperature was assumed to be equal when the heater of the bearing gas was off; it was also measured using the BVT 1000 thermocouple and proved to be 0.5 K lower than room temperature.

Si_3N_4 and ZrO_2 rotors were packed under inert gas with a 7 mm layer of NaCl at the bottom of the rotor, followed by a 4 mm layer of a mixture of Cp_2V and Cp_2Fe and a second 4 mm layer of NaCl in order to reduce temperature gradients^{2h-j} in the paramagnetic sample and to keep the weight of different rotors as constant as possible. Macor caps provided excellent mechanical stability of the rotor and long-term stability of the sample.

Spectra were recorded at 5 K intervals with temperature equilibration times of 30 and 45 min for Si_3N_4 and ZrO_2 rotors, respectively. Typical recording times were 3.2 min for a ^1H and 1.5 h for a ^{13}C NMR spectrum. Cp_2V^4 and Cp_2Fe were sublimed and mixed (20% w/w of Cp_2Fe) in a mortar under inert gas; co-sublimation gave a sample that contained approximately 40% of Cp_2Fe . The $\text{Cp}_2\text{Co}/\text{Cp}_2\text{V}/\text{Cp}_2\text{Fe}$ sample was prepared similarly by combining the standard mixture of $\text{Cp}_2\text{V}/\text{Cp}_2\text{Fe}$ (85:15) with freshly sublimed Cp_2Co in the ratio 3:7. Ethylene glycol and TTMSS used for calibration were distilled from sodium and recrystallized from ethanol, respectively, and a Si_3N_4 rotor was prepared as described previously.^{2f} The calibration of the MAS probe-head was based on the data obtained in solution¹³ and recalculated for 300 MHz ^1H NMR ($T_s = 466.5 - 0.338\Delta\nu$, where $\Delta\nu$ is the distance in Hz between the CH_3 and OH resonances of glycol). The correlation between T_s and T_c was determined with the glycol-TTMSS sample for two rotor spinning rates: $T_s = 0.9159T_c + 23.55$ at 2.1 kHz and $T_s = 0.8761T_c + 36.59$ at 6.0 kHz. The constant term may change with the ambient temperature, which was

297.5 K in the present study. The 6 kHz temperatures series was repeated after routine use of the spectrometer otherwise for 1 week, and the same T_s – T_c correlation was found within the experimental error. The curves depended on ν_c as described for $\text{Cp}_2\text{V}/\text{Cp}_2\text{Fe}$.

The temperature calibration of $\text{Cp}_2\text{V}/\text{Cp}_2\text{Fe}$ in toluene solution was carried out by using a high-resolution $^{13}\text{C}/^1\text{H}$ dual probe accommodating 5 mm tubes. The resulting correlation [Eqn (1)] was in good agreement with the results obtained by Dietrich and co-workers:⁹ $T = 9.346 \times 10^4 \delta^{\text{para}}(^1\text{H}) + 0.55$ (eight data points for $293.27 \text{ K} \leq T \leq 363.15 \text{ K}$, $r = 0.9999$).

The FIDs for both the ^1H and ^{13}C nuclei were obtained from standard single-pulse experiments with a

repetition time of 500 ms; the digital resolution was 28 Hz per point. The data were processed by using WIN NMR, version 95; reverse linear prediction proved to be advantageous for reliable phase correction and proper baselines.

Acknowledgement

We are indebted to Drs W. Strauss and H. Hilbig for performing the solution-state measurements, to Dr W. Dietrich for communicating his results to us and to Professor A.-R. Grimmer for a preprint. We also express our gratitude to the Alexander von Humboldt Foundation for a fellowship (X.-L.X.) and the Fonds der Chemischen Industrie for financial support.

REFERENCES

1. J. F. Haw, G. C. Campbell and R. C. Crosby, *Anal. Chem.* **58**, 3172 (1986).
2. (a) T. Bjornholm and H. J. Jakobsen, *J. Magn. Reson.* **84**, 204 (1989); (b) B. Wehrle, F. Aguilar-Parrilla and H.-H. Limbach, *J. Magn. Reson.* **87**, 584 (1990); (c) H. Pan and B. C. Gerstein, *J. Magn. Reson.* **92**, 618 (1991); (d) C. P. Grey, A. K. Cheetham and C. M. Dobson, *J. Magn. Reson. A*, **101**, 299 (1993); (e) K. L. Anderson-Altmann and D. M. Grant, *J. Phys. Chem.* **97**, 11096 (1993); (f) A. E. Aliev and K. D. M. Harris, *Magn. Reson. Chem.* **32**, 366 (1994); (g) G.-J. M. P. van Moorsel, E. R. H. van Eck and C. P. Grey, *J. Magn. Reson. A*, **113**, 159 (1995); (h) L. C. M. van Gorkom, J. M. Hook, M. B. Logan, J. V. Hanna and R. E. Wasylshen, *Magn. Reson. Chem.* **33**, 791 (1995); (i) A. Bielecki and D. P. Burum, *J. Magn. Reson. A*, **116**, 215 (1995); (j) T. Mildner, H. Ernst and D. Freude, *Solid State Nucl. Magn. Reson.* **5**, 269 (1995); (k) F. G. Riddell, R. A. Spark and G. V. Günther, *Magn. Reson. Chem.* **34**, 824 (1996); (l) A.-R. Grimmer, A. Kretschmer and V. B. Cajipe, *J. Magn. Reson.* **35**, 86 (1997); (m) D. B. Ferguson and J. F. Haw, *Anal. Chem.* **67**, 3342 (1995).
3. J. Blümel, M. Herker, W. Hiller and F. H. Köhler, *Organometallics* **15**, 3474 (1996).
4. F. H. Köhler, in *Organometallic Synthesis*, edited by R. B. King and J. J. Eisch, Vol. 4, p. 15. Elsevier, Amsterdam (1988).
5. H. Eicher, F. H. Köhler and R. Cao, *J. Chem. Phys.* **86**, 1829 (1987), and references cited therein.
6. E. König, V. P. Desai, B. Kanellakopulos and E. Dornberger, *J. Organomet. Chem.* **187**, 61 (1980).
7. A. Nayeem and J. P. Yesinowski, *J. Chem. Phys.* **89**, 4600 (1988); C. P. Grey, C. M. Dobson, A. K. Cheetham and R. J. B. Jakeman, *J. Am. Chem. Soc.* **111**, 505 (1989).
8. E. Oldfield, R. A. Kinsey, K. A. Smith, J. A. Nichols and R. J. Kirkpatrick, *J. Magn. Reson.* **51**, 325 (1983).
9. (a) W. Dietrich and M. Pliennisch, unpublished results; M. Pliennisch, Dissertation, Universität Bochum (1991); (b) W. Dietrich and H. Ulbrich, unpublished results; H. Ulbrich, Dissertation, Universität Bochum (1996).
10. F. H. Köhler, *Z. Naturforsch., Teil B* **35**, 187 (1980).
11. A. M. James and M. P. Lord, *Macmillan's Chemical and Physical Data*, p. 438. Macmillan, London (1992).
12. F. Aguilar-Parrilla, B. Wehrle, H. Bräunlig and H.-H. Limbach, *J. Magn. Reson.* **87**, 592 (1990).
13. A. L. Van Geet, *Anal. Chem.* **40**, 2227 (1968); D. S. Rainford, C. L. Fisk and A. E. D. Becker, *Anal. Chem.* **51**, 2050 (1979).